

REFERENCES

1. Laevskiy Yu.M., Babkin V.S. Filtration combustion // Thermal wave distribution in heterogeneous media / Ed. by Yu.Sh. Matros. – Novosibirsk: Nauka, 1988. – P. 108–145.
2. Dae Ki Min, Hyun Dong Shin. Laminar premixed flame stabilized inside a honeycomb ceramic // Int. J. Heat mass transfer. – 1991. – V. 34. – № 2. – P. 341–356.
3. Aldushin A.P., Merzhanov A.G. The theory of filtration combustion: General ideas and the research state // Thermal wave distribution in heterogeneous media / Ed. by Yu.Sh. Matros. – Novosibirsk: Nauka, 1988. – P. 9–52.
4. Oliveira A.A.M., Kaviany M. Nonequilibrium in the transport of heat and reactants in combustion in porous media // Progress in Energy and Combustion Science. – 2001. – V. 27. – № 5. – P. 523–545.
5. Martynenko V.V., Echingo R., Yoshida R. Mathematical model of self-sustaining combustion inert porous medium with phase change under complex heat transfer // Int. J. Heat mass transfer. – 1998. – V. 41. – № 1. – P. 117–226.
6. Henneke M.R., Ellzey J.L. Modeling of filtration combustion in a packed bed // Combustion and flame. – 1999. – V. 117. – № 4. – P. 832–840.
7. Barra A.J., Diepvens G., Ellzey J.L., Henneke M.R. Numerical study of the effects on flame stabilization in a porous burner // Combustion and Flame. – 2003. – V. 134. – № 4. – P. 369–379.
8. Trimis D., Durst F., Pickencker O., Pickencker K. Porous medium combustion versus combustion systems with free flames // In: Advances in Heat Transfer Enhancement and Energy Conservation [C]. Guangzhou: South China University of Technology Press, 1998. – P. 339–345.
9. Kirdyashkin A.I., Maksimov Yu.M. Infrared burner on the basis of porous ceramics // Energy saving and energy efficiency: The materials of the reports of the VIII International exhibition-congress. – Tomsk, 2005. – P. 24–25.
10. Isserlin A.S. The bases of gas fuel combustion: Reference book. – Leningrad: Nedra, 1987. – 336 p.
11. Ksandopulo G.I. Chemistry of flame. – Moscow: Khimiya, 1980. – 256 p.

Received on 20.12.2006

UDC 636.468+536.3

IGNITION OF POROUS HIGH-ENERGY SUBSTANCES BY LIGHT RADIATION

A.N. Subbotin

Tomsk Polytechnic University
E-mail: subbot@inbox.ru

The possibility of calculation of high-energy solid fuel ignition processes within the limits of the porous reacting body model has been shown. Using the given model of ignition, it is possible to consider the dependence of ignition time on pressure which is ascertained experimentally while within the limits of the classic solid-phase ignition theory the ignition time does not depend on the initial and the external pressure.

As the experimental investigations show [1–3], the process of ignition of solid fuels (SF) is accompanied by various physical phenomena, in particular: SF gasification with heat release; the gasification products motion in pores; homogeneous chemical reactions in the condensed phase. At the same time the existing «solid-phase» (heterogeneous) and gaseous ignition theories are to some extent limiting and do not consider the whole variety of physical phenomena connected with SF ignition. For example in [4, 5] the solid-phase ignition model is used. Applying it the minimum sizes of heated bodies capable of igniting solid fuel are determined. In this work the above listed processes are taken into account in the development of solid phase ignition model within the frames of the model of porous reactive medium [6]

The reactive medium is supposed to be one-temperature; in the condensed phase the only effective homogeneous reaction of the form $v_1M_1 \rightarrow v_2M_2 + v_3M_3$, where v_1M_1 is the mass of the initial condensed substance (SF) occurs; v_2M_2 , v_3M_3 is the mass of condensed and gaseous

products of SF combustion reaction. The flux equal q_e falls from the external radiation source to the fuel surface. Gaseous products motion in pores and heat-mass exchange of fuel with the environment are taken into account. Let us study the ignition mechanism and determine the ignition time.

The equation system [6] describing the concerned process is written down in dimensionless form

$$\frac{\partial \varphi_1}{\partial t} = -\gamma_1 \varphi_1 \exp \frac{\theta}{1 + \beta \theta},$$

$$\frac{\partial (\rho \varphi_3)}{\partial t} + \frac{\partial (\rho \varphi_3 u)}{\partial x} = \gamma_3 \varphi_1 \exp \frac{\theta}{1 + \beta \theta}, \quad (1)$$

$$c_{ps} \frac{\partial \theta}{\partial t} + \rho \varphi_3 c_p u \frac{\partial \theta}{\partial x} = \frac{\partial}{\partial x} \left(\lambda_s \frac{\partial \theta}{\partial x} \right) + \varphi_1 \exp \frac{\theta}{1 + \beta \theta}, \quad (2)$$

$$u = -g \pi_u \frac{\partial p}{\partial x}, \quad p = \frac{\rho (1 + \beta \theta)}{\pi_p}, \quad g = \frac{\varphi_3^3 (1 - \varphi_3)^{-2}}{\sqrt{1 + \beta \theta}}. \quad (3)$$

This system was solved at the following boundary conditions

$$\rho \Big|_{\tau=0} = \rho_n, \varphi_i \Big|_{\tau=0} = \varphi_{in}, \theta \Big|_{\tau=0} = -\theta_n, u \Big|_{\tau=0} = 0, \quad (4)$$

$$u \Big|_{x=\infty} = 0, \theta \Big|_{x=\infty} = -\theta_n, (\rho \varphi_3 u)_{x=0} = -\pi_g (p_w - p_e), \quad (5)$$

$$\lambda \frac{\partial \theta}{\partial x} \Big|_{x=0} = -\bar{\sigma} [\varepsilon_e (1 + \beta \theta_e)^4 - \varepsilon_w (1 + \beta \theta_w)^4]. \quad (6)$$

The notations: $c_p = c_{p3}/c_{p1}$, $\rho = \rho_3/\rho_1$, $u = v/v_n$, $p = P/P_n$ the dimensionless specific heat, density, filtration rate and pressure of gaseous products in pores, respectively; $c_{ps} = \varphi_1 + \alpha_2 \varphi_2 + \rho \varphi_3$ is the dimensionless heat of the reactive medium; $g = k\mu/k_n\mu$ is the dimensionless function which has the form (3), if the formula of Kozeny-Carmen [7] for the coefficient of permeability k , Darcy, is used; μ is the absolute viscosity coefficient, kg/(m·s); $\pi_u = k_s p_s c_{p1} \rho_1 / \lambda_1 \mu_n$, $\pi_g = \alpha_m E L_n / (\lambda_1 R)$, $\pi_p = p_n M_3 / (\rho_1 R T_n)$, $\beta = RT_n / E$, $\alpha = \rho_2 c_{p2} / (\rho_1 c_{p1})$, $\gamma_3 = \gamma_1 v_3 M_3 / (v_1 M_1)$, $\gamma_1 = c_{p1} \rho_1 R / (qE)$, $\bar{\sigma} = \sigma E L_n / \lambda_1 R$ are the dimensionless parameters; $\lambda = \varphi_1 + \varphi_2 \lambda_2 / \lambda_1 + \varphi_3 \lambda_3 / \lambda_1$ is the dimensionless heat conductivity coefficient of porous agent; $\theta = E(T - T_n) / (RT_n^2)$ is the dimensionless temperature; $L_n = [\lambda_1 R T_n^2 \exp(E/RT_n) / (qk_0 E \rho)]^{0.5}$ is the distance scale, m; $t_n = c_{p1} R T_n^2 \exp(E/RT_n) / (qk_0 E)$ is the time scale, s; $x = y/L_n$, $\tau = t/t_n$ are the dimensionless coordinate and time; $u = v/v_n$ is the dimensionless filtration rate; R is the universal gas constant, J/(mole·K); $\varphi_1, \varphi_2, \varphi_3, \rho_1, \rho_2, \rho_3, c_{p1}, c_{p2}, c_{p3}, \lambda_1, \lambda_2, \lambda_3$ are the volume ratio, density, specific heat and heat conductivity coefficient of SF, condensed and gaseous reaction products, respectively; q, k_0, E is the thermal effect, pre-exponential factor and combustion reaction activation energy, J/kg, 1/s, J/mole; σ is the Stefan-Boltzmann constant, W/(m²·K⁴); θ_e, θ_w is the dimensionless temperature of irradiation source and SF surface, respectively; $\varepsilon_e, \varepsilon_w$ is the emissivity factor of the radiator and heating surface; q_e is the luminous flux density, W/m² are introduced here.

The boundary problem (1)–(6) was numerically solved at use of iterated-interpolation method [6]. As a result of numerical solution of this problem it was determined that there are three ignition stages differing from each other. According to [8] the explosive permeability changes in the range of (10⁻²...10⁻⁶) Darcy. The data on permeability of a concrete SF was not found out in scientific literature therefore, the initial permeability k_n was taken equal 10⁻⁶ Darcy. The other parameters were taken for powder H from the works [3, 9] $T_n = 550$ K, $\lambda_1 = 0,302$ W/(m·K), $qk_0 = 4,2 \cdot 10^{17}$ J/(kg·s), $P_n = 1$ atm $c_{p1} = 1257$ J/(kg·K), $E = 117,6$ J/mole, $\rho_1 = 1866$ kg/m³. We obtain $t_n = 8,6 \cdot 10^{-3}$ s, $L_n = 3,5 \cdot 10^{-5}$ m at the given constant values.

Fields of pressure, temperature and rate of filtration for two time points $\tau = 92$ (curves 1) and $\tau = 302,1$ (curves 2) are introduced in Fig. 1, 2, a.

The results introduced in these Figures are obtained at $\pi_g = 5,8 \cdot 10^{-4}$, $\theta_n = 11,64$, $\varphi_{in} = 0,85$, $\varphi_{3n} = 0,05$, $\beta = 0,04$, $\gamma_1 = 0,01$, $p_n = 10$ atm, $p_e = 150$ atm. Radiant heat flux q_e was assigned equal $8,4 \cdot 10^4$ W/m² that is confirmed to the experimental data of the works [3, 10]. Analyzing the diagrams of Fig. 1, b, we draw the conclusion that the peak temperature for this ignition stage is always at the bo-

dy surface (on media interface). As it follows from Fig. 2, a, the filtration rate in this case has the dissection point скорость (the point in which the filtration rate direction changes), and curve $\theta_w(\tau)$ for ignition stage (Fig. 2, b) has the inflexion point. Rapid temperature rise of the surface $\theta_w(\tau)$ at $\tau > 290$ is conditioned by the intensive heat release from chemical reaction and indicates the reacting agent ignition.

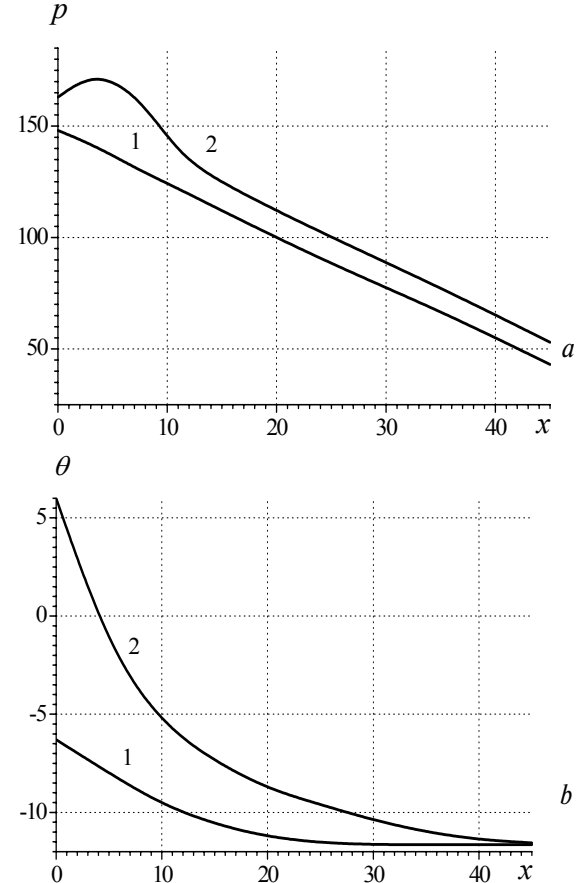


Fig. 1. Profiles of: a) pressure and b) temperature in porous fuel at ignition

At numerical calculations the ignition was considered to occur if $\theta_w(\tau) \geq 1$. The condition $\theta_w(\tau) \geq 5$ may be used instead of this condition etc. Analyzing Fig. 2, b, we draw the conclusion that the ignition time determined by the first inequality differs slightly from the ignition time determined by the second inequality. However, if the condition

$$d^2 \theta_w / d\tau^2 \Big|_{\tau = \tau_p} = 0,$$

where τ_p is the time corresponding the inflexion point of the curve $\theta_w(\tau)$ is used for determining the ignition time then τ_p found out by this condition differs considerably from the ignition time. Therefore, the empirical criterion of ignition of the form $\theta_w(\tau) \geq \theta_g$, where θ_g is the constant greater than or equal unit is appropriate to be used for determining the ignition time.

It should be noted that till the ignition time the pressure in pores decreases at increase of the coordinate x and the formed gaseous products are pushed into the fu-

el and after ignition ($\tau \geq \tau_p$) the pressure peak inside the ignited fuel layer is formed (Fig. 1, *a*, curve 2), and the outflow of the formed gaseous products into environment starts (Fig. 2, *a*, curve 2). Therefore, agent ignition in this case should be called the ignition in the mode of forced injection. At ignition in the mode of forced injection the peak value of burning at the ignition time amounts about 30 % and implemented in the narrow band at heating surface.

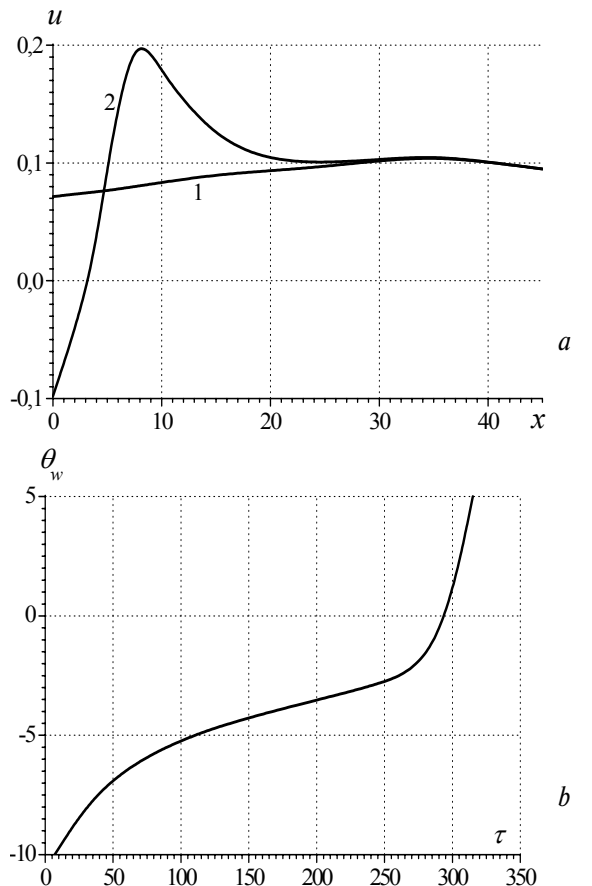


Fig. 2. Depth change of porous SF layer: *a*) filtration rate of *b*) time dependence of surface temperature at ignition

If the pressure in the external medium equals the pressure in solid fuel layer, for example, $p_e = p_n = 70$, $\pi_g = 5,8 \cdot 10^{-7}$, and the other parameters are the same then the ignition stage, differs qualitatively from the previous one, takes place. In Fig. 3, 4, *a*, for two time points $\tau = 1207,2$ (curves 1) and $\tau = 1058$ (curves 2) the profiles $p(x)$, $\theta(x)$ and $u(x)$ are introduced. It is seen that functions $p(x)$ and $\theta(x)$ before the ignition time are the monotone decreasing function x .

It should be noted that monotony of the function $p(x)$ up to the ignition moment for this mode is explained not by the increased external pressure but by a very slight mass-exchange with the environment. Owing to the negligibly low mass exchange with the environment almost all formed gaseous products are pushed deep inside the ignited fuel. In this connection this mode of ignition should be called the ignition stage at low intensity of the external mass exchange.

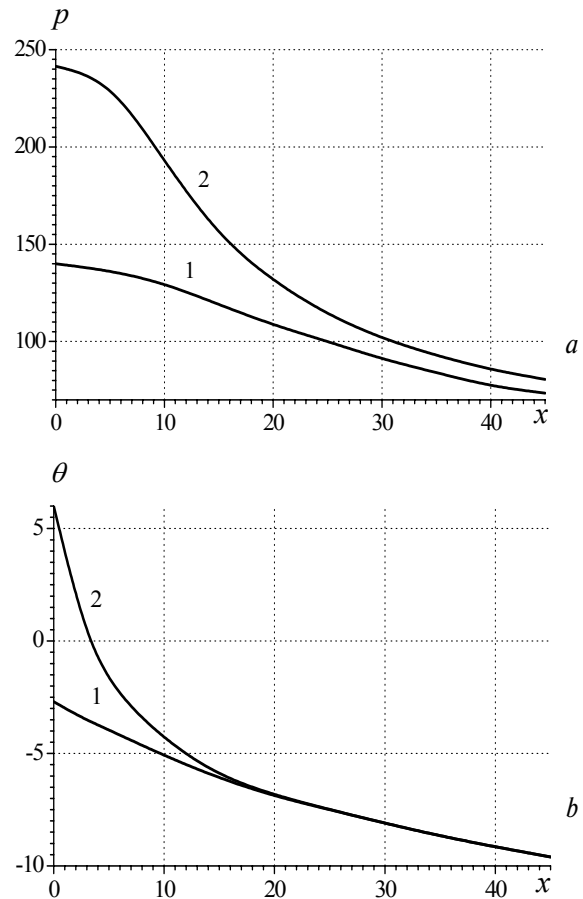


Fig. 3. Profiles of: *a*) pressure and *b*) temperature before (curves 1) and after (curves 2) SF ignition by luminous flux at slight mass-exchange with the environment

Along with this mode the ignition at medium or strong external mass exchange is possible. It should be noted that within the frame of this ignition stage the injection rate is considerably higher than in those considered before. In particular, in Fig. (4, *b*, 5) the filtration rates, fields of pressure and temperature which are obtained at $p_e = p_n = 10$ atm, $\pi_g = 5,8 \cdot 10^{-4}$ and previous values of other parameters are introduced; here curves 1 correspond to the time point $\tau = 667,3$, and curves 2 – $\tau = 787,2$.

Analyzing these Figures the conclusion may be drawn that at the given ignition stage a rather large pressure gradient is formed inside the studied layer (Fig. 5, *a*), a comparatively intensive filtration of gaseous products both to the external medium and inside the layer occurs (Fig. 2, *a*, and Fig. 4). The filtration rate at the intensive mass exchange with the environment is higher by an order than in previous two ignition stages. If the considered ignition stages are compared by the depth of fuel decomposition and ignition time τ_g , then it should be noted that the ignition time and dimensionless depth of decomposition H are minimum $\tau_g \approx 300$, and $H \approx 7$ for ignition in the forced injection mode. $\tau_g \approx 1600$, and $H \approx 12$ for the ignition stage with low intensity of the external mass exchange. Finally, at the ignition with medium or high mass exchange with the environment the ignition

time $\tau_g \approx 780$, and the dimensionless depth of decomposition $H \approx 19$.

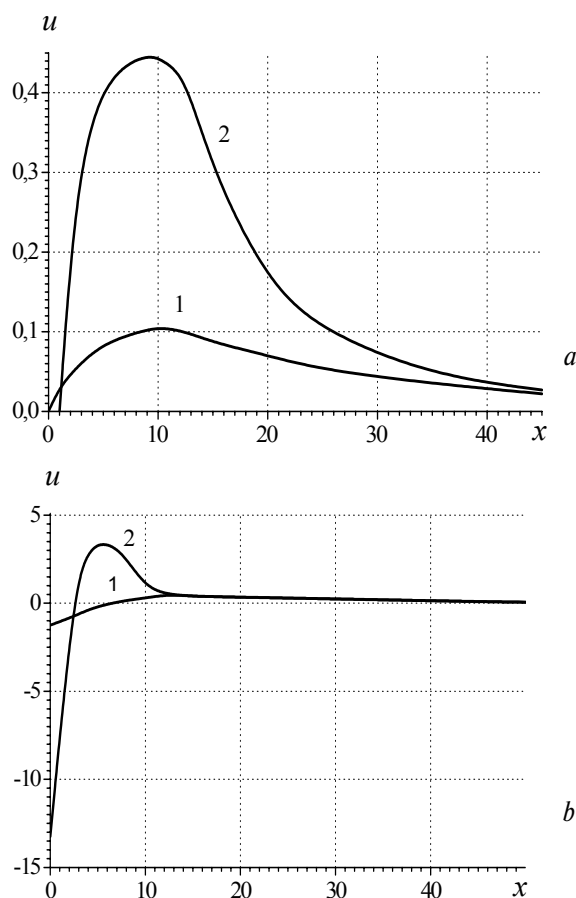


Fig. 4. Spatial distribution of filtration rate at: a) weak and b) intensive mass-exchange with the environment

The main characteristic interesting for practitioners is the ignition time. In this connection the investigation of the influence of the heat flow rate q_e and heat exchange on the surface on ignition time is of interest. The dependences of ignition time on radiant heat flux are introduced in fig. 6. The results given in this Figure were obtained at $\theta_n = 11,64$, $\varphi_{n1} = 0,85$, $\varphi_{n2} = 0,05$, $\beta = 0,04$, $\gamma_1 = 0,01$, $p_n = 70$ atm, $p_e = 70$ atm, $k_n = 10^{-6}$ Darcy, $\gamma_3 = 0,5\gamma_1$, $T_* = 550$ K. On the basis of the analysis of the dependences in Fig. 6, a, the conclusion may be drawn that at growth of the parameter π_g , i.e. at intensification of gaseous product injection through the pores the ignition time increases significantly. This effect is conditioned by carry over certain amount of energy together with gaseous products blown out the pores. It is interesting that for each value π_g there is its own threshold q_{e*} , the ignition does not occur (the ignition time tends to infinity) lower it and q_{e*} increases at π_g growth.

Let us further examine the influence of the external and initial pressure in pores on the ignition time. In Fig. 6, b, the dependences $t_g = f(q_e)$, which are obtained at $\pi_g = 5,8 \cdot 10^{-4}$ are shown; the other parameters are the same as for the Fig. 6, a. Comparing the dependences 1 and 2, the conclusion is drawn that at pressure growth in the mode of medium or intensive mass exchange the ig-

nition time decreases at $q_e < 22 \cdot 10^4$ W/m², and increases if $q_e > 22 \cdot 10^4$ W/m². This effect is conditioned obviously by the fact at lower pressure inside the layer at increase of the external heat flow the convective energy transport deep inside the layer due to filtration of gaseous products becomes higher than at higher pressure. This conclusion follows from the analysis of the dependence 3 of Fig. 6, b, in which the ignition time decreases in the mode of forced injection ($p_e > p_n$) at other equal conditions (curves 2 and 3).

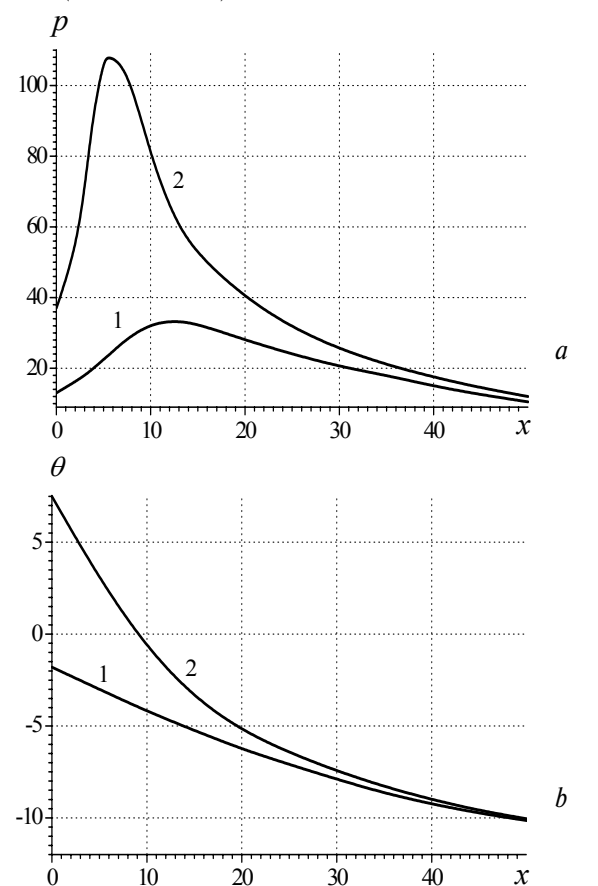


Fig. 5. Pressure spatial distribution (a) and warmed up layer depth (b) at intensive heat exchange with the environment

It was ascertained by the numerical calculations that the ignition time increases in the mode of the intensive mass exchange at growth of the parameter γ_3 characterizing gas formation. The dependences of the ignition time on q_e for two threshold cases are introduced in Fig 7, a. The curve 1 is obtained at $\gamma_3 = 0$ (there is no gas formation till the ignition time), and curves 2 and 3 at $\gamma_3 = \gamma_1$ (the condensed substance turns fully to gaseous one).

The parameter π_g was specified equal $5,8 \cdot 10^{-4}$ (the mode of intensive mass transfer), $p_e = p_n = 10$ atm, and the other parameters were the same (as for the Fig. 5) for dependences 1 and 2. If we specify $\pi_g = 5,8 \cdot 10^{-6}$, then at $\gamma_3 = \gamma_1$ the dependence 3 in Fig. 7, a is obtained. Therefore, the increase of gas formation rate influences differently the ignition time. At intensive mass exchange on the surface the ignition time increases (energy is carried away with the blown out gas) and at low mass exchange

the ignition time decreases owing to filtration of the reaction hot products deep inside the fuel. As the numerical calculations showed, the ignition time decreases considerably at γ_3 growth in the mode of forced injection.

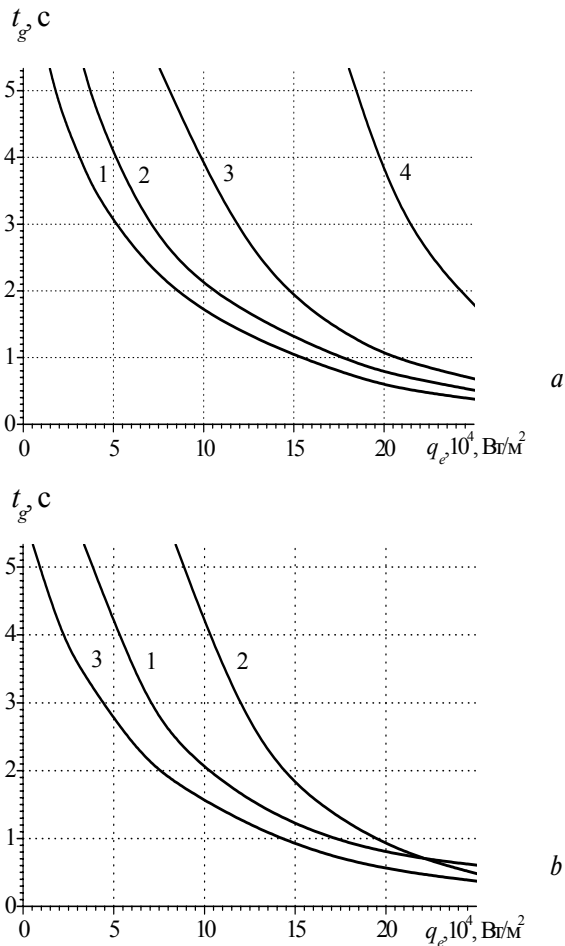


Fig. 6. The dependence of ignition time (a) on luminous flux density for different conditions of mass exchange with the environment: 1) $\pi_g=0$, 2) $\pi_g=5,8 \cdot 10^{-6}$, 3) $\pi_g=1,3 \cdot 10^{-5}$, 4) $\pi_g=5,8 \cdot 10^{-3}$ and at different values of pressure (b): 1) $p_e=p_n=200$ atm, 2) $p_e=p_n=10$ atm, 3) $p_e=150$ atm, $p_n=10$ atm

The ignition time depends directly and indirectly on porosity as permeability is the function of porosity. The dependences of the ignition time on initial porosity at $\theta_n=11,64$, $k_n=10^{-6}$ Darcy, $p_n=p_e=70$ atm, $\beta=0,04$, $\gamma_1=0,01$, $\gamma_3=0,5\gamma_1$, $\pi_g=5,8 \cdot 10^{-4}$ are introduced in Fig. 7, b. Here the curve 1 corresponds to $\varphi_{3n}=0,05$, and curve 2 – $\varphi_{3n}=0,15$. It follows from the Figure that at increase of φ_{3n} at the same initial permeability the ignition time grows as the intensity of heat generation source decreases. At the same time, if the dependence of permeability

on porosity is taken into account then the ignition time falls at increase of φ_{3n} . For example, at one and the same luminous flux $q_e=16,8 \cdot 10^4$ W/m^2 and other parameters $\theta_n=11,64$, $p_n=p_e=70$ atm, $\beta=0,04$, $\gamma_1=0,01$, $\gamma_3=0,5\gamma_1$, $\pi_g=5,8 \cdot 10^{-6}$, if $\varphi_{3n}=0,05$, $k_n=10^{-6}$ Darcy then the ignition time equals 0,78 s and if $\varphi_{3n}=0,1$, $k_n=5 \cdot 10^{-4}$ Darcy then $t_g=0,36$ s.

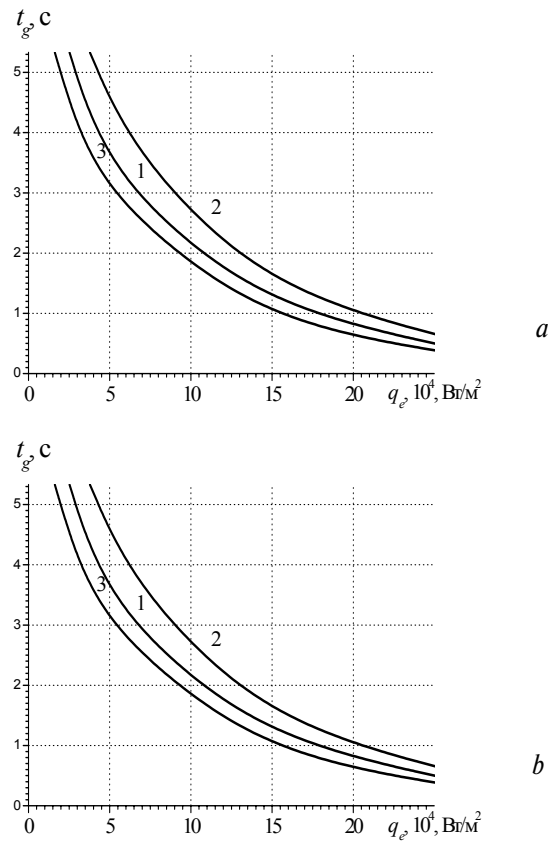


Fig. 7. Dependence of the ignition time on luminous flux value at: a) different conditions of gas formation and b) different porosity

Thus, within the frame of this model of condensed substance ignition a satisfied (from physical point of view) explanation of the ignition time dependence on pressure may be given; while within the frame of classical solid-phase theory of ignition [11–13] the ignition time does not depend on initial and external pressure.

In conclusion it should be noted that the ignition times obtained at solution of this problem coincide by an order of magnitude with the known experimental data, for example [3, 10]. Quantitative coincidence of theoretical computation and experimental data may be easily obtained determining the empirical constant π_g experimentally at ignition of concrete high-energy substances.

REFERENCES

1. Khlevnoy S.S., Kalmykov A.P. Firing nitroglycerin powder with light in cold gas flow // Physics of combustion and explosion. – 1968. – V. 4. – № 1. – P. 122–124.
2. Price Bredly, Deority Ibritsu. The solid fuel ignition theory// Rocket engineering and astronautics. – 1966. – № 1. – V. 3–41.
3. Mikheev V.F., Kovalskiy A.A., Khlevnoy S.S. Ballistit powder light ignition // Physics of combustion and explosion. – 1968. – V. 4. – № 1. – P. 3–9.
4. Isakov G.N., Sandrykina T.S., Subbotin A.N. Heat exchange and critical conditions of VEV ignition by heated bodies of finite sizes // Fundamental and applied problems of modern mechanics: All-Russian scientific conference. Materials of the reports. – Tomsk: Tomsk State University Press, 2002. – P. 297–298.
5. Isakov G.N., Subbotin A.N., Sandrykina T.S. On VEV ignition at shielding penetration by high-speed compact body // The third Okunvskie readings: International research practice conference. Materials of the reports. – Saint-Petersburg: BGTU Press, 2004. – V. 2. – P. 77–80.
6. Grishin A.M., Zinchenko V.I., Subbotin A.N. et al. Iterated-interpolation method and its supplements. – Tomsk: Tomsk State University Press, 2004. – 319 p.
7. Polubarinova-Kochina P.Ya. The theory of groundwater motion. – Moscow: Nauka, 1977. – 664 p.
8. Belyaev A.F., Bobolev V.K., Korotkov A.I., Sulimov A.A., Chui-ko S.V. Transition of the condensed system combustion into explosion. – Moscow: Nauka, 1973. – 292 p.
9. Kovalskiy A.A., Khlevnoy S.S., Mikheev V.F. On the issue of ballistit powder ignition // Physics of combustion and explosion. – 1967. – V. 3. – № 4. – P. 527–541.
10. Mikheev V.F., Khlevnoy S.S. Pyroxylin ignition by light radiation // The second All-Union symposium on combustion and explosion (abstracts of the reports). – Chernogolovka, 1969. – P. 9–10.
11. Averson A.E., Barzykin V.V., Merzhanov A.G. Regularities of condensed explosive system ignition at the ideal heat exchange on the surface subject to burning out // Engineering-physical review. – 1965. – V. 9. – № 2. – P. 245–249.
12. Merzhanov A.G., Averson A.E. The Present State of the Thermal Ignition Theory // Combustion and Flame. – 1971. – V. 16. – № 1. – P. 89–124.
13. Merzhanov A.G. Theory of Stable Homogeneous Combustion of Condensed Substances // Combustion and Flame. – 1968. – V. 13. – № 4. – P. 421–434.

Received on 08.12.2006

UDC 536.46

ON THE THEORY OF EROSIVE BURNING OF SOLID ROCKET FUELS

K.O. Sabdenov, O.Yu. Dolmatov

Tomsk Polytechnic University
E-mail: sabdenovko@mail.ru

The explanation of the erosive burning threshold presence has been offered. It is shown that such kind of burning begins at decrease in thickness of the laminar sublayer (in a turbulent boundary layer) below width of the laminar burning zone. The expressions connecting critical (threshold) rate of the blowing stream and critical number of V.N. Vilyunov with properties of fuel and gas formed at its decomposition are obtained. Simple power dependences on blowing stream rate are found for burning rate.

Introduction

Further improvement of Russian nuclear-missile board requires, besides development of up-to-date nuclear military loads, the efficient carriers – the rocket system, as well; in particular, rocket engine on solid fuel. One of significant elements in this issue is the detailed appreciation of fuel charge burning laws and production of improved methods for their accounting at engine construction and calculation of rocket target flight dynamics.

Among the majority of factors (fuel burning nonstationarity, stability etc.) there is an effect of erosive burning. It is known [1, 2] that such kind of burning refers to the group of threshold phenomena and appears as increase of burning rate u under the action of burning blowing the surface with hot gas flow. It occurs, as a rule, at excess of average (or maximal) gas rate w_∞ along burning surface of critical value w^* . If the burning rate is denoted by u_w at erosive effect then one of widely used expression (for bounded variation interval w_∞) for u_w has the form:

$$u_w = u[1 + k_e (w_\infty - w^*)], \quad w \geq w^*;$$

$$u_w = u, \quad w_\infty < w^*; \quad k_e = \text{const.}$$

Numerical constant k_e is called the erosion factor. At the early stages of studying, specialists did not pay attention to threshold character of erosive burning. Therewith, the physics of the phenomenon itself was not clear.

In the theory of V.N. Vilyunov [3] inner mechanism of erosion effect consists in intensification of heat, pulse and mass transfer processes in burning zone of gas phase under the influence of turbulence. Overall it results in growth of heat flow from chemical reaction zone in gas phase to fuel decomposition surface increasing its temperature T_s . As a result, burning rate grows as well. The (criterion) number of Vilyunov acts here as the principle parameter determining the process

$$J = \sqrt{C_f} \frac{\rho w_\infty}{\rho_c u},$$